

MODELING THE ACCUMULATION OF SECONDARY CRATERS ON MARS AND THE MOON. T. M. Powell¹ (tylerpowell@ucla.edu), L. Rubanenko², J.-P. Williams¹, and D. A. Paige, University of California, Los Angeles, CA, USA, ²Stanford University, Stanford, CA, USA.

Introduction: The relative importance of secondary craters on the accuracy of crater chronology has been debated since the 1960s¹. Some individual primary craters have been shown to produce $\sim 10^6$ - 10^9 secondary craters which form nearly instantaneously in geologic time^{2,3,4,5}. This is a complication for crater chronology, which relies on the predictable accumulation of craters following a knowable size-frequency distribution (SFD) and rate. The effect of secondary craters on crater chronology can be determined if the flux of primaries and the size-frequency and spatial distribution of the secondaries they create are known.

In this work, we address the over-arching questions: What size craters can be used reliably for crater counting? How does this vary spatially and with surface age? To do this, we: 1) use a global catalog of Martian and Lunar craters to constrain the size-frequency and spatial distribution of secondaries produced by several large primaries; and 2) model secondary accumulation with time, accounting for spatial clustering.

Characterization of secondary SFDs: Several large (~ 100 km-scale) primary craters on Mars and the Moon show enhancements in the spatial density of 1-10 km craters in their nearby regions^{6,7,8,9}. To characterize the secondary population around these primaries, we use a global crater catalog^{7,8} to compare a secondary-containing region to a nearby reference region of similar age and geology. Subtracting the SFDs between these two regions results in a distribution of “excess” craters which we assume to be secondaries. An advantage of this approach is that it is agnostic to classification criterion like morphology or clustering.

Figure 1 shows examples of two Martian craters with noticeable secondary fields. The distribution of excess craters is fit to a power-law: $N_s = (fD_p)^{b_s} D^{-b_s}$ where b_s is the power-law slope and the coefficient is expressed in terms of size of the largest secondary, fD_p . For four Martian craters, we find values of b_s ranging from ~ 3.7 - 4.3 , consistent with previous studies^{1,6}. However, we require an f of ~ 7 - 12% to explain the number of excess craters. This is greater than the 5% value which has been used in previous studies^{10,11}.

To characterize the drop-off of secondaries with distance, we fit the radial profile of excess crater spatial density using a power-law with exponent, α . For Lomonosov crater, we find a relatively rapid drop-off with distance ($\alpha \sim 4.5$). For Lyot, we find a more gradual drop-off ($\alpha \sim 2.9$), though this may be influenced by the degradation of nearby secondaries.

Model Description: Previous authors have modeled the global secondary SFD by summing the contributions from each primary^{1,4,9,10,11}. However, this approach does not account for spatial clustering, which is necessary for determining the number of field secondaries in areas not clearly influenced by nearby large primaries.

We develop a model which accounts for the spatial distribution of secondary craters⁹. Primary craters are stochastically placed on a surface according to the Ivanov PF¹², and each primary produces secondaries based on parameters f , b_s , and α . The surface is gridded, and the spatial density and crossover diameter (the diameter at which secondaries exceed primaries) within each bin are calculated.

Results: Figure 2 shows model results for Mars. After 1 Ga, secondaries exceed primaries by an order-of-magnitude globally. However, most secondaries are contained within a few crater radii of the largest several primaries, and a typical/median surface contains far fewer secondaries than the global mean would suggest (figure 2B). We predict that the median crossover diameter after 1 Ga may be as large as 300 m (figure 2C), significantly lower than the global mean of ~ 6 km. For surfaces younger than ~ 100 Ma, we predict a median crossover diameter of < 10 m, about the limit of what can easily be counted using existing orbital imagery. The median crossover diameter is expected to exceed 1 km after ~ 1 - 2 Ga.

This model represents a production population and does not account for crater erasure. However, erasure has significantly influenced the number of secondaries visible today: Lyot crater has the most prominent secondary field for a > 200 km crater on Mars⁶, despite there being ~ 50 craters of similar size or larger on the Martian surface. As a result, our model likely provides an overestimate to the current-day secondary population and median crossover diameter. Because of the high spatial variability of secondaries, care should be taken when counting craters on the scale of or smaller than the expected crossover diameter.

References: [1] Shoemaker (1965) *The Nature of the Lunar Surface*, 23-77. [2] Bierhaus et al. (2001) *Icarus*, 153(2), 264-276. [3] Dundas and McEwen (2007) *Icarus*, 186(1), 31-40. [4] McEwen et al. (2005) *Icarus*, 176(2), 351-381. [5] Williams (2018) *Dynamic Mars*, 365-386. [6] Robbins and Hynes (2011) *JGRP*, 116(E10). [7] Robbins and Hynes (2012) *JGRP*, 117(E5). [8] Robbins (2019) *JGRP*, 124, 871-892. [9] Powell et al. (2021, In press) *Mars Geological Enigmas*. [10] Soderblom et al. (1974) *Icarus*, 22(3), 239-263. [11] Werner et al. (2009) *Icarus*, 200(2), 406-417. [12] Ivanov (2001) *Space Sci. Rev.*, 96(1-4), 87-104.

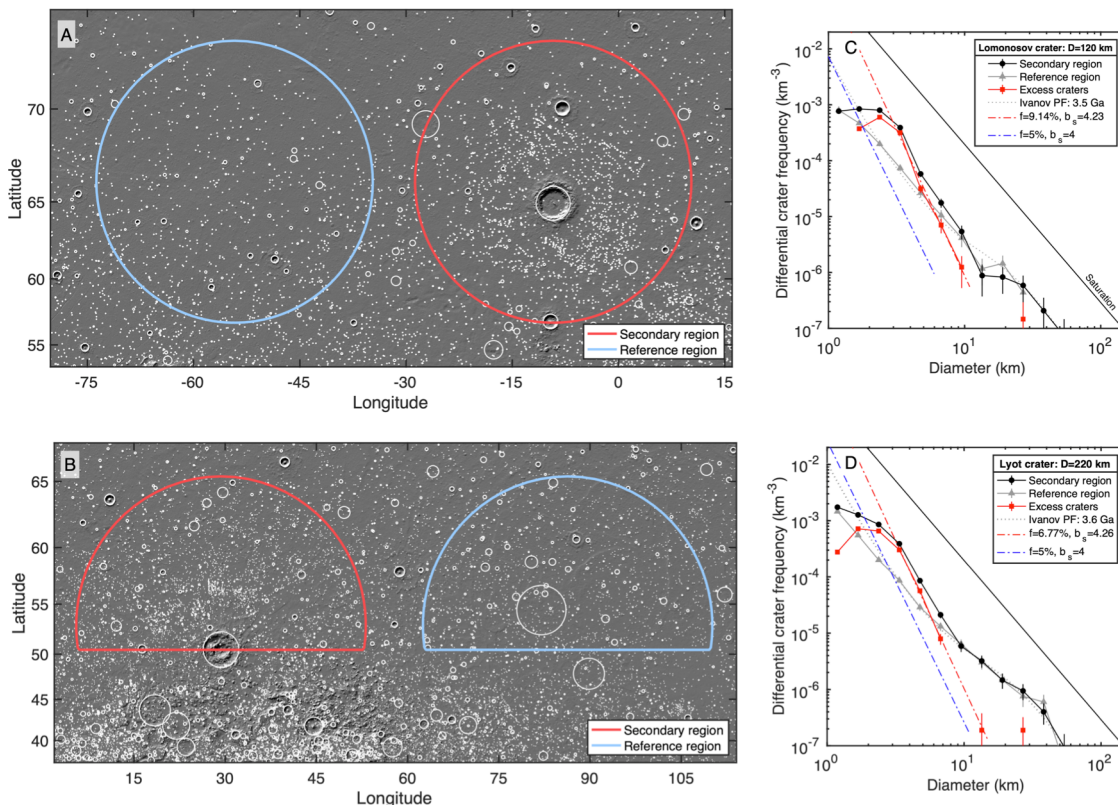


Figure 1. All craters larger than 1 km in the region around (A) Lomonosov crater (120 km) and (B) Lyot crater (220 km) from the Robbins and Hynek (2012) Martian crater catalog⁷. We consider a region extending to 8 crater radii. For Lyot, we only consider the northern half of this annulus due to a change in terrain type to the south. (C and D) Differential crater SFDs in the region around Lomonosov and Lyot compared to the SFD of a nearby reference region. The SFD of excess craters is fit using a power-law.

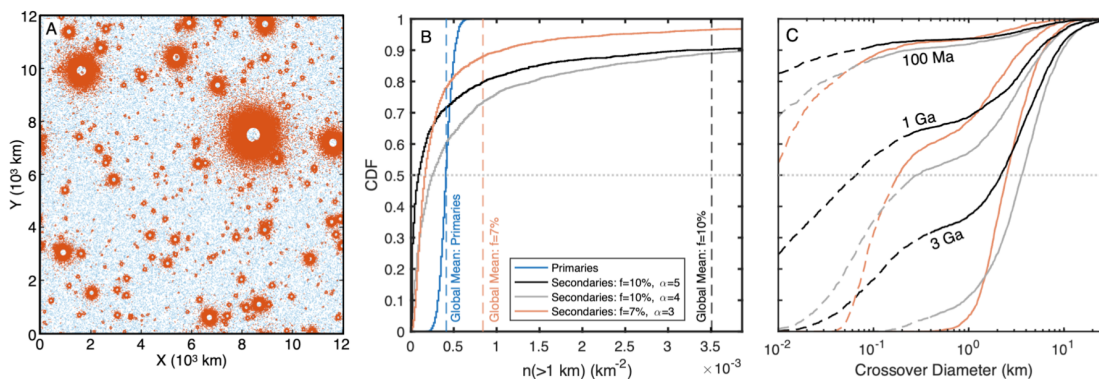


Figure 2. (A) Example of a simulated map of primary and secondary craters for a Mars-sized surface after 1 Ga ($f = 0.1$, $b_s = 4$, and $\alpha = 5$). (B) Cumulative histogram of the spatial density of primary and secondary craters after 1 Ga for various model parameters. The spatial density of primaries is centered around the global mean. However, most secondaries are clustered around large primaries and the median secondary spatial density (indicated by a CDF of 0.5) is significantly lower than the global mean. (C) Cumulative histogram of the local crossover diameter at various times. The dashed line indicates when that crossover diameter requires the largest primary to produce more than 10^8 secondaries.